Journal of the Energy Institute 93 (2020) 1460–1472

Contents lists available at ScienceDirect

Journal of the Energy Institute

journal homepage: www.journals.elsevier.com/journal-of-the-energy-institute

Study of devolatilization during chemical looping combustion of large coal and biomass particles

K. Sekar Pragadeesh [a], Iyyaswami Regupathi [a], D. Ruben Sudhakar [a, b, *]

[a] Department of Chemical Engineering, National Institute of Technology Karnataka, Surathkal, Mangalore, 575025, India
[b] Department of Energy and Environment, National Institute of Technology, Tiruchirappalli, 620015, India

ARTICLE INFO

Article history:
Received 14 August 2019
Received in revised form
1 January 2020
Accepted 6 January 2020
Available online 9 January 2020

Keywords:
Chemical looping combustion
Devolatilization
Char yield
Shape effect

ABSTRACT

Chemical Looping Combustion (CLC) is one of the emerging technologies for carbon capture, with less energy penalty. The present way of using pulverized coals in a fluidized bed (FB)-CLC have limitations like loss of unconverted char and gaseous combustibles, which could be mitigated by use of coarser fuel particles. Devolatilization time is a critical input for the effective design of FB-CLC systems, primarily when large fuel particles are used. The present study investigates the devolatilization time and the char yield of three coals of two shapes, namely, two high ash Indian coals and a low ash Indonesian coal and a wood (*Casuarina equisetifolia*) in the size range of +8–25 mm, at different fuel reactor temperatures (800 –950 °C) of a hematite based CLC unit. The devolatilization times of single fuel particles during CLC are determined using a visual method called 'Color Indistinction Method'. Indonesian coal has the longest devolatilization time among the fuels, and biomass has the least. Increasing the bed temperature enhances the rate of volatile release, whereas this effect is less pronounced in larger particles. Devolatilization of Indonesian coal is found to be strongly influenced by the changes in operating conditions. With the decrease in sphericity, a maximum of 56% reduction in devolatilization time is observed for the +20 –25 mm slender particles of Indonesian coals when compared to the near-round particles. The maximum average char yields at the end of the devolatilization phase for coal and biomass are about 55 –76% and 16% respectively. Char yield in coal particles increases with an increase in particle size, whereas biomass particles show relatively consistent yield across all experimental conditions. Increase in bed temperature reduces the char yields of coal up to 12% and in biomass up to 30%. High volatile Indian coal is the most influenced fuel by the changes in fuels shape. A correlation for determining devolatilization time under CLC environment is presented, and it successfully fits most of the experimental values within ±20% deviation for coals ($R^2 = 0.95$) and within ±15% deviation for biomass ($R^2 = 0.97$).

1. Introduction

Carbon dioxide, a greenhouse gas emitted into the atmosphere from various sources, is one of the most significant contributors to global warming. The energy sector, particularly thermal power plants, is the largest anthropogenic source of carbon emissions, where coal is the major feedstock. Biomass, which is a carbon-neutral fuel finds application in co-firing, with coal as the primary fuel. Several carbon capture technologies are currently being investigated to mitigate the effect of global warming [1–4]. Among them, in-situ capture methods are found to be more efficient [4–6]. Chemical Looping Combustion (CLC), an in-situ carbon capture technology is gaining importance in the recent years due to its good potential of getting commercialized [4,7]. CLC is considered to be the technology with the least energy penalty on plant efficiency [6,8]. It generally uses a two-reactor system, i.e., an air reactor and a fuel reactor. The oxidation of fuel is achieved by employing an oxygen carrier material, typically a metal oxide which is looped between these two reactors. CLC with fluidized bed (FB) is a widely used configuration due to the better gas-solid mixing in FB reactors [9]. Circulating Fluidized Beds (CFBs) are preferred type of fuel reactor for gaseous fuels, whereas, bubbling fluidized beds (BFBs) are preferred as fuel reactors for solid fuels [6,10–12]. The advantage of BFBs over CFBs for solid fuels lies in the longer residence times of fuel particles, which ensure the complete conversion of

* Corresponding author. Department of Energy and Environment, National Institute of Technology, Tiruchirappalli, 620015, India
E-mail address: rubensudhakar@nitt.edu (D.R. Sudhakar).

https://doi.org/10.1016/j.joei.2020.01.008
1743-9671/

char by preventing the loss of carbon out of the reactor. Based on the oxygen carrier used, CLC can be classified into iG-CLC (insitu Gasification-CLC), CLOU (Chemical Looping with Oxygen Uncoupling) and CLaOU (CL assisted by Oxygen Uncoupling) [4]. The solid fuel is gasified initially in all the cases, and the combustible gases react with oxygen carrier in iG-CLC to form CO_2 and H_2O [13], whereas CLOU fastens the oxidation process by providing nascent oxygen from oxygen carriers [14]and CLaOU uses mixture of iG-CLC and CLOU materials [4].

Gaseous fuels like methane, syngas are studied extensively in CLC research. Since 2008, CLC of solid fuels like coal, biomass, pet coke, sewage sludge is being investigated [15]. Until now, solid fuels are tested in pulverized forms (micron sized) only. Pulverisation being an energy-intensive operation will further increase energy penalty for fuels like high ash Indian coals and biomass. Moreover, CLC being a relatively slow process compared to conventional combustion processes, use of pulverized coal in CLC have drawbacks like escape of unconverted char to air reactor as well as into the exit stream, possible release of unconverted combustibles into exit stream (which would require separate oxygen polishing step) and require carbon separation units [16]. Using coarse fuel particles have advantages like longer fuel particle residence time, avoidance of oxygen polishing step, and reduction in pulverisation cost [7]. These advantages favor the use of high ash Indian coals and biomass in larger sizes (mm range). Though fluidized beds could accommodate usage of fuel particles in wide size range, effective and conservative design of these combustors would require inputs such as fuel devolatilization time, char combustion time, fragmentation behavior and volumetric changes in fuel particle during conversion [17].

Devolatilization is the initial phase of a solid fuel conversion process wherein the volatile matter gets released from fuel particle. Regarding CLC technology, when the fuel feed particle sizes are very small (micron-sized), devolatilization occurs spontaneously in fraction of a second which is mostly released above the oxygen carrier bed and in consequence, the oxygen/oxygen-carrier demand increases proportionally. Berguerand et al. [18] reports that unconverted volatiles in freeboard contributes to 75% of the oxygen demand created in the fuel reactor, where the particles size ranged from 90 to 250 μm. Ideally, the oxygen carrier demand can be met by supplementing the inventory which would result in increased reactor volume and require additional power for fluidization. These facts suggest the requirement of better mixing of oxygen carrier and volatiles, which can be achieved by providing more residence times to fuel particles. The micron sized particles easily get carried over to air reactor and exhaust stream, owing to their low mass compared to oxygen carrier. Thus, it becomes very important to hold the fuel particles in the oxygen carrier bed during most of the fuel conversion regime and particularly during the devolatilization time. As mentioned earlier, coarser millimetre-sized particles release volatiles at a gradual pace and provide longer residence time. When the feed particle size is larger, the heat required to release the volatiles reach the particle centre at different times depending on the particle size. This is attributed to the fact that the influence of heat transfer on the fuel particle [19–21] comes into picture in addition to the chemical reaction kinetics control when the particle size exceeds 0.6 mm [22,23] or thermally thick, as is the case in the present study. Thus, the studies on rate of devolatilization and the associated char yields are of significance in the conversion of mm-sized solid fuel particles using CLC technology.

Devolatilization time of fuel samples is affected by other parameters such as bed temperature, shape, and fuel properties. When devolatilization is accompanied by thermal fragmentation, it further influences the heat and mass transfer between the fuel and the reactor environment. It also becomes essential to study the effect of the shape of coal particles on the devolatilization time since the industrial feed particles are irregularly shaped with a wide range of sphericity. The present study is aimed at determining the devolatilization time and char yield of large fuel particles (mm-sizes) of three different coals and woody biomass in FB-CLC and analyzing the influence of operating parameters over them. In a first of its kind of study, the effect of changes in particle sphericity arising out of size reduction of coal particles on devolatilization is also investigated.

2. Experimental

The experiments are conducted in a batch mode fluidized bed CLC unit which is shown in Fig. 1 [24], which is used in an earlier work by Pragadeesh and Sudhakar [24]. It is comprised of a cylindrical column with an internal diameter of 130 mm and height of 600 mm, fluidized with the aid of a porous distributor plate with orifice opening of 2 mm. A bed aspect ratio of 1 is maintained throughout the experiments. An overboard provision of stainless-steel mirror is employed for visualizing in-bed events. Air is used as the fluidizing and oxidizing agent during intermittent air reactor mode for oxygen carrier regeneration and steam is the fluidizing cum gasification agent during the fuel reactor mode. Two Indian coals (IC1, IC2), Indonesian coal (IDC) and biomass are chosen for this study. A locally sourced hematite is used as the oxygen carrier. The properties and composition of the fuel and the oxygen carrier, are detailed in Tables 1 and 2 respectively, which are the same as reported in our previous work [24].

The devolatilization experiments are conducted at three different bed temperatures, namely 800, 875 and 950 °C. The coal particles are tested in three different sizes (8–25 mm range), and two shapes, i.e., near-rounded and flake particles as formed out of crushing and sieving operation. The sizes of fuel particles are expressed in terms of mass equivalent diameters as well as in sieve opening size ranges, wherever necessary. Biomass cubes of 10, 15 and 20 mm are used in the experiments.

Devolatilization times of the fuel samples are determined by Color Indistinction Method [25]. In Color Indistinction Method (CIM), the devolatilization time of the fuel particle is determined based on the color change of the particle surface from black to reddish orange. The end time of devolatilization is marked by the disappearance of reddish-orange fuel particles in the red-hot fluidizing bed. The samples are retrieved immediately at the end of devolatilization time using a stainless-steel mesh basket and subsequently quenched to prevent char oxidation. The char yield is calculated based on the mass retained by the fuel particles after the devolatilization time experiment.

3. Results and discussion

The devolatilization time (τ_d) of various coals used in this study and the operating parameters influencing the devolatilization time are discussed in their order of influence (high to low). Generally, devolatilization processes are controlled by following processes [21,22,26–28] inside the combustor, namely.

i. Intensity or the rate of heat transfer from the surroundings to the surface of the fuel particle
ii. Variation in thermal properties of the fuel which results in a temperature gradient within the fuel particle
iii. Kinetics of chemical reaction during devolatilization
iv. Resistance to the viscous flow or mass diffusion from inside of the particle core towards the surface, through the porous structure in fuel.

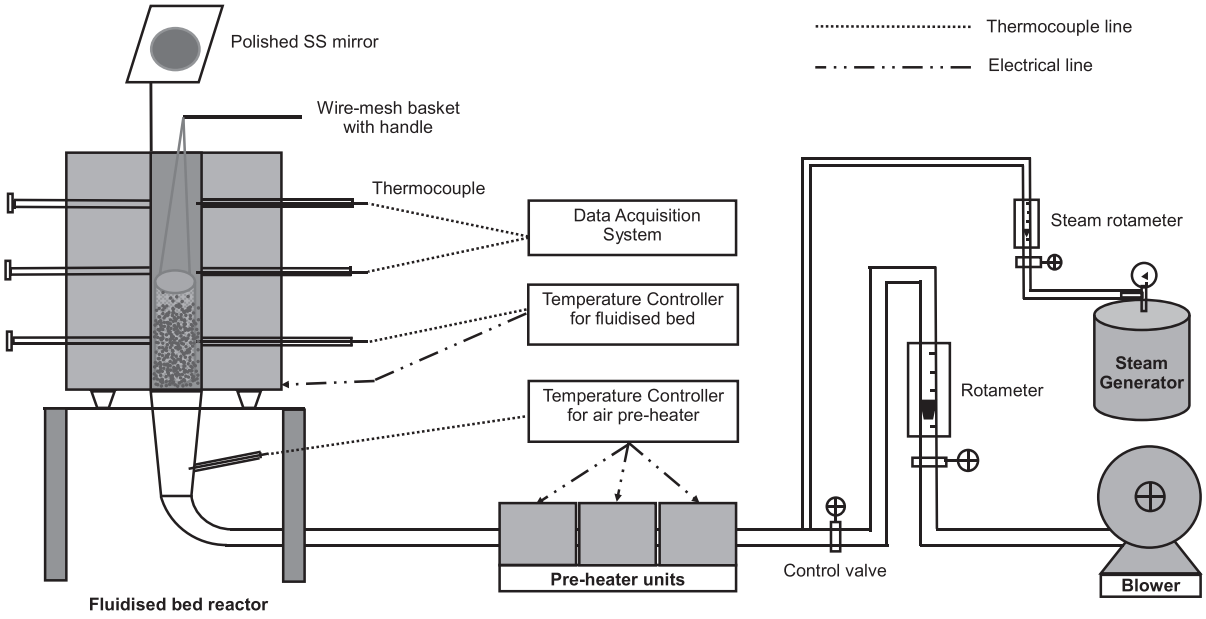

Fig. 1. Schematic of the experimental setup used in this study [24].

Table 1
Properties and compositions of fuels used.

Composition (%wt.)	Indian Coal 1 (IC1)	Indian Coal 2 (IC2)	Indonesian Coal (IDC)	Biomass (BM)
Moisture	8.2	4.5	6.3	8.9
Volatile Matter	33.5	23.2	40.4	79.8
Fixed Carbon	31.9	29.62	43.62	10.9
Ash	26.4	42.68	9.68	0.4
Elements (%wt.)				
Carbon	53.53	43.62	60.74	43.76
Hydrogen	2.133	1.86	5.01	5.69
Nitrogen	0.64	1.04	0.89	0.16
Oxygen	8.98	5.88	17.18	41.02
Property				
Bulk density (kg/m^3)	702	939	647	780
Particle density (kg/m^3)	1480	1917	1274	-

The effect of temperature gradient and flow filtration on devolatilization can be noticed along with the changes in particle size. The effect of heat transfer intensity is associated with bed temperature variation. Influence of temperature gradient on the devolatilization process is also related to the fuel type, where density differences are the primary causes. The devolatilization time and the char yield of four different fuels with varying sample parameters (size, sphericity) at different bed temperatures are reported and discussed. Additional data points have been drawn from Pragadeesh and Sudhakar [25] for Indian coal IC2 and biomass (BM) for comparison purposes.

3.1. Effect of the type of fuel

The nature of fuel is the most significant factor influencing its devolatilization behavior. The devolatilization times of different fuels of different sizes studied at different bed temperatures are given in Fig. 2.

Table 3 shows the magnitude of devolatilization time with the combination of mineral matter and volatile matter. Among the coal types studied, the fuel with the highest volatiles content i.e. IDC takes more time to release the volatiles completely. Coals with higher volatile content have higher specific heat capacity [29], and this may be one of the reasons why IDC takes more time to acquire heat and devolatilize. Compared to other fuel particles, biomass particles rapidly devolatilize at any given temperature. The difference in the devolatilization time between coals and biomass arise because of the mineral matter present in them, i.e., more the mineral content, higher the devolatilization time [30]. One other important component which affects the devolatilization time is fixed carbon content. It can be noticed that the devolatilization time increases with the increase in fixed carbon content.

Among all the fuel types studied, IDC has the highest devolatilization times, and biomass has the least devolatilization times for different particle sizes. From Fig. 2, the following observations are made.

Table 2
Characteristics of oxygen carrier (iron ore).

Physical properties						
Bulk density (kg/m3)			2186			
Particle density (kg/m3)			4541			
Mean particle diameter (μm)			337.5			
Chemical composition						
Composition	LoI*	Fe(T)$^+$	SiO_2	Al_2O_3	P	Mn
Mass %	4.80	62.43	1.20	2.25	0.151	1.01

*Loss on Ignition, $^+$Total Iron.

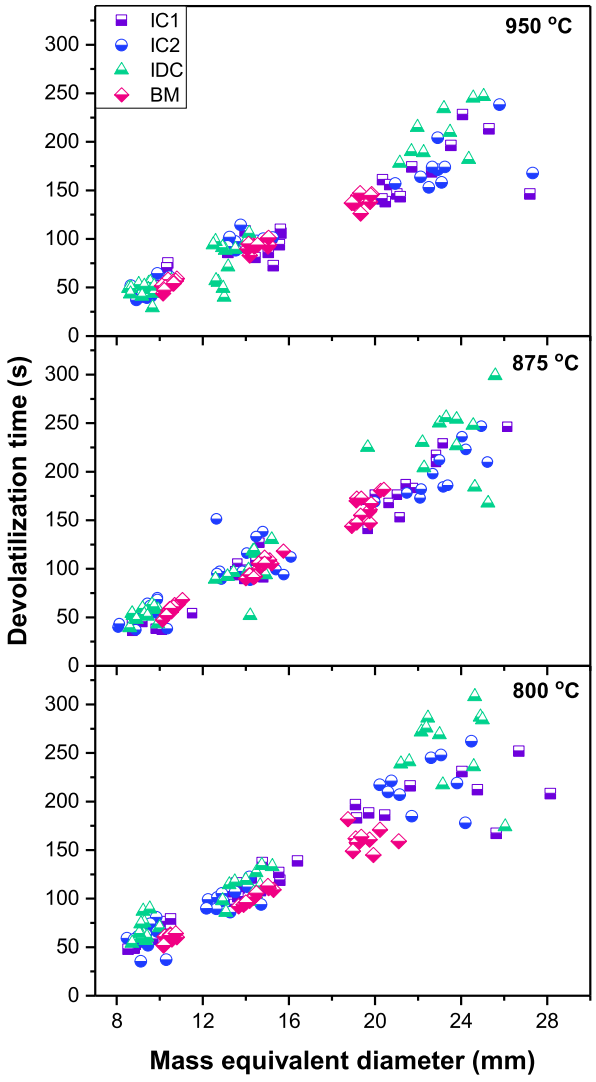

Fig. 2. Scatter plot of devolatilization time showing the influence of the fuel type at different bed temperatures.

Table 3
The magnitude of devolatilization time based on the composition of various fuels.

Fuel	Magnitude of devolatilization time	Composition
IDC	Highest	● high VM, FC and low MM
IC1	High	● medium VM, FC and low MM
IC2	Low	● low VM, FC and highest MM
BM	Lowest	● highest VM and lowest FC, MM

Note: MM – Mineral Matter; VM – Volatile Matter; FC – Fixed Carbon.

(i) Fuel with a high mineral matter and volatile content takes more time to devolatilize.
(ii) Fuel with low mineral matter and high volatiles content devolatilize very quickly.

As mentioned earlier, for the fuels with low volatile content, the scattered trend of devolatilization time is seen. The Indian coals are seen to have more scattered data points, which may be either due to the heterogeneity or the structural deformations leading to reduced devolatilization times. As expected, the IDC and biomass particles have clustered data points for a given size range, which can be explained by the relatively inherent homogenous nature of the fuels. At 950 °C, the scatter among the largest sized particles is reduced, which may be owing to the predominant crack formation or the fragmentation events occurring alongside the devolatilization process of the fuel particles. In addition to fragmentation, higher temperatures favor tar cracking [31], resulting in a faster rate of volatile release.

3.2. Influence of particle size on devolatilization time

The devolatilization times of the two Indian coals, Indonesian coal and biomass studied at three different bed temperatures, for various particle sizes are given in Fig. 3. The dotted curves indicate the trend of devolatilization time with the increase in particle size. Across all temperatures studied, the coal particles have τ_d in the range of 23–89 s for +8–10 mm sizes, 56–139 s for +12.5–16 mm sizes and 102–309 s for +20–25 mm sizes. The biomass particles have τ_d of 44–68 s for 10 mm, 83–118 s for 15 mm and 126–182 s for 20 mm cubes.

All the coal types exhibit an increasing trend of devolatilization time with respect to particle size (represented in terms of particle diameter), irrespective of the bed temperatures studied (Fig. 3). The particles in the smallest size range studied (9 mm) do not show much difference in their devolatilization time of the same/nearer particle size. As the size increases, the spread between the devolatilization times of the various samples of the same size range increases and observed to be highest in case of the largest particle sizes (22.5 mm) studied. This spread is attributed to the effect of increased heterogeneity as well as to the effect of varying thermal conductivity towards the innermost core from the surface, as the particle size increases, i.e. from a zone of ash skeleton to a zone of ash with fixed carbon. As the particle size increases, the distance and time taken by viscous volatile matter also increase. During this process, the tarry volatiles may not get released completely due to the secondary reactions within the pore structure succeeding the competition with the intraparticular volatile convection [26,32,33]. Instead, they get settled over various regions in the flow path of volatiles in the fuel particle, causing resistance to the mass flow, which further reduces the rate of heat transfer towards the particle center. Consequently, internal heat transfer becomes predominant, resulting in increased devolatilization time. Wood particles exhibit similar devolatilization characteristics as that of coal particles. Devolatilization behavior of the fuels in the CLC environment is apparently similar to the case of the conventional FB combustion processes [31,34]. However, the order of magnitude of τ_d is relatively higher in CLC environment when compared to conventional air combustion [25]. The observations indicate the longer residence time of fuel particles, which is essential for the proper conversion of volatile matter released. Particularly, the larger particles exhibit the advantages of gradual release of volatiles, as noticed by the increase in slope of devolatilization trend line (Fig. 3).

Comparison of devolatilization times of the Indian coals and Indonesian coal reveals a relatively larger scatter among the data points of Indian coals. This spread is due to the effect of different degrees of heterogeneity existing between the particles within the same size range [25]. Heterogeneity among fuel particles within the same size range and across sizes may be due to one or more of the following characteristics of the fuels.

(i) Difference in amount of volatile matter present in individual particles.
(ii) Distribution of mineral matter interspersed with the carbon framework.
(iii) Structural variations developed during the formation of the fuel chunk.

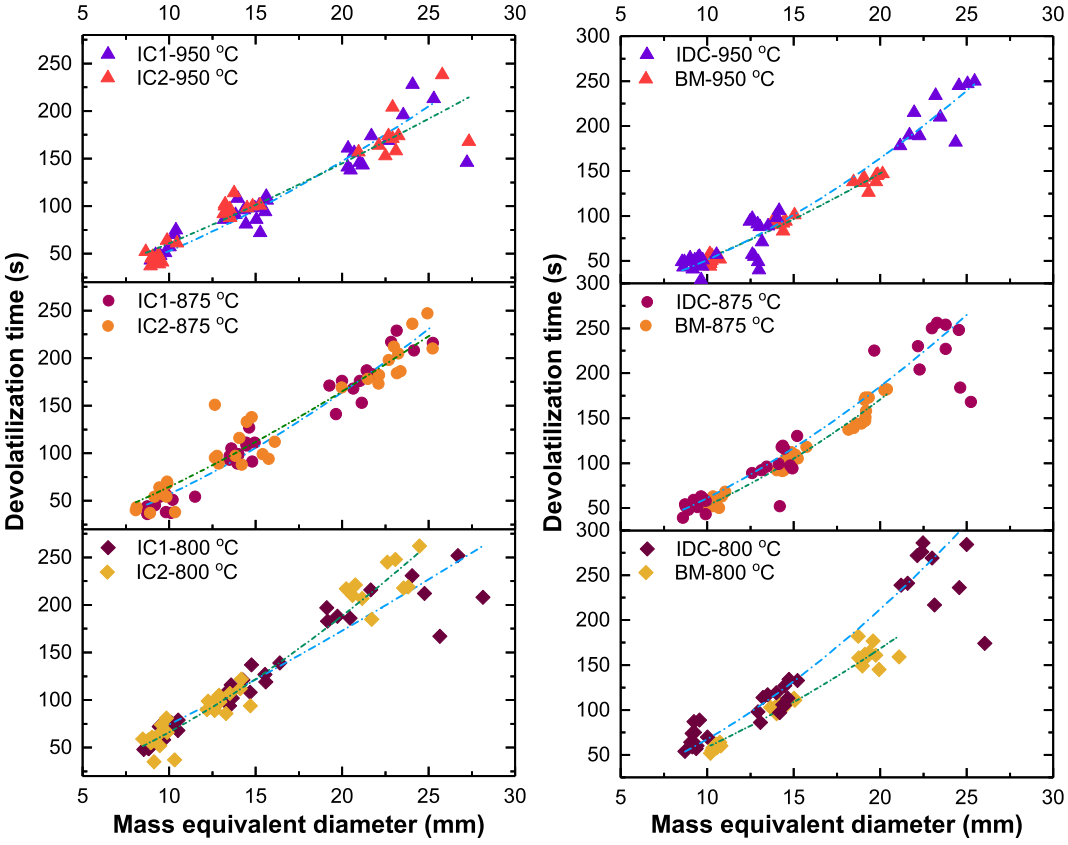

Fig. 3. Devolatilization times of different fuels with varying particle sizes.

Within the Indian coals, the coal with relatively higher volatile content (IC2) has a comparatively higher slope of the devolatilization trend, and the slope of IDC is the highest among the coals, which has the highest volatile matter among them. However, at the same time, biomass has a significantly different trend (relatively lower slope than IDC), despite having more volatiles. The difference in the rates of devolatilization is due to the relatively less dense and high porous nature of the fuel. In detail, the volatiles generated at high temperatures in a biomass particle faces relatively less obstruction to get liberated, due to the porous nature of the fuel. Whereas, the denser coal particles have a gradual volatile release towards the surface of the particle due to the resistance to the mass transport created by the mineral matter as well as the fixed carbon matter, which makes them less porous.

The ratio of devolatilization time of the largest to the smallest sized particles is calculated using the average devolatilization times at each bed temperature and the range of values are given (Table 4). The broader range of devolatilization time ratio of the largest particle to the smallest particle is found with IC1 and IDC has the least range. On average, the devolatilization time of coals increases by four to five folds when particle size is increased from 8 mm to 25 mm. Biomass particles have a narrow range in the devolatilization time ratio and have about a 3-fold increase in devolatilization time with the increase in particle size from 8 mm to 25 mm. From this observation, it can be drawn that if a fuel has a broader range of this ratio, more the fuel heterogeneity and the effect of bed temperature. As Indian coals have wider ratios, they behave inconsistently and influences the reactor conditions, such as rate of fuel feeding and ash retrieval, leading to tedious material handling. Relatively, the low ash biomass and IDC are easier to handle.

Table 4
The ratio of devolatilization times of largest to smallest particles used across different bed temperatures.

Fuel	Ratio of devolatilization time (largest to smallest size)
IC1	2.9–4.4
IC2	4.4–5.7
IDC	4.8–5.1
BM	2.8–3.6

3.3. *Effect of operating bed temperature*

The effect of bed temperature on the devolatilization time of the fuels studied is presented in Figs. 4 and 5. For all the fuels, the devolatilization time decreases with increase in temperature, which is a trend observed in the literature on fuel devolatilization in conventional FBCs [21] as well as in CLC studies [35–38] using micron sized particles. The temperature effect is evinced clearly with every type of fuel studied, being prominent in larger particles compared to smaller. It implies that the heat transfer is slowed down by the presence of mineral matter and the fixed carbon, as discussed in section 3.2.

In terms of percentage reduction in τ_d with an increase in bed temperature from 800 to 950 °C, biomass particles experience the least effect, having a reduction of only 10–14% for all sizes. Coal samples show a decrease of 11–27% in τ_d for smaller sizes but a lesser reduction of 15–22% in case of the 22.5 mm particles. This kind of behavior with coal particles is observed earlier in conventional combustion environments [39], where the effect of bed temperature on volatile evolution is less pronounced in larger particles. This can be directly attributed to highly competitive

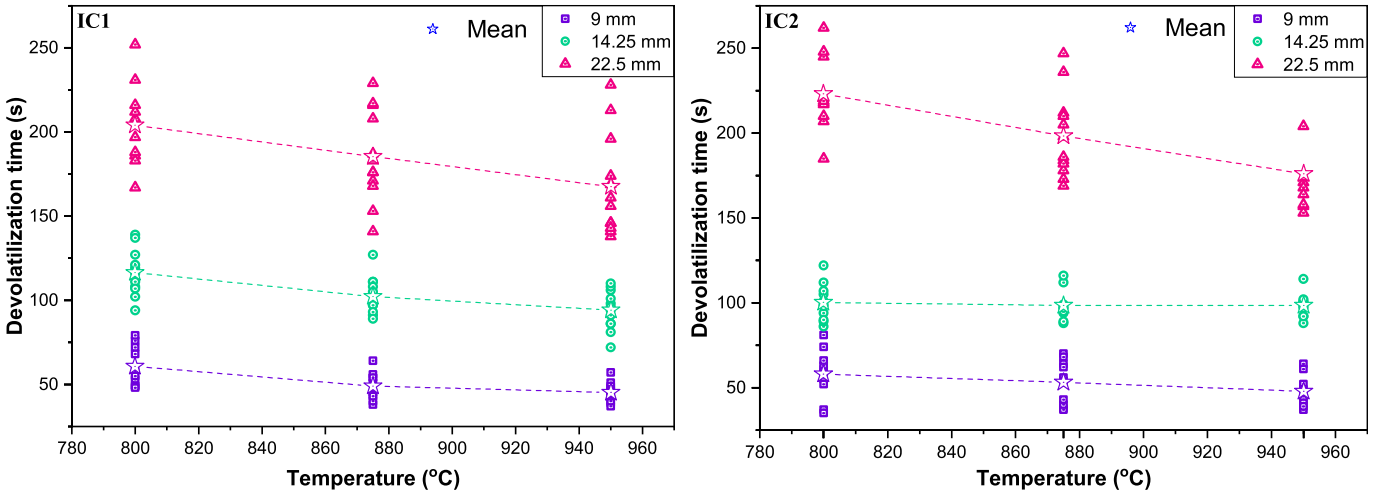

Fig. 4. Devolatilization time of IC1 and IC2 at different bed temperatures.

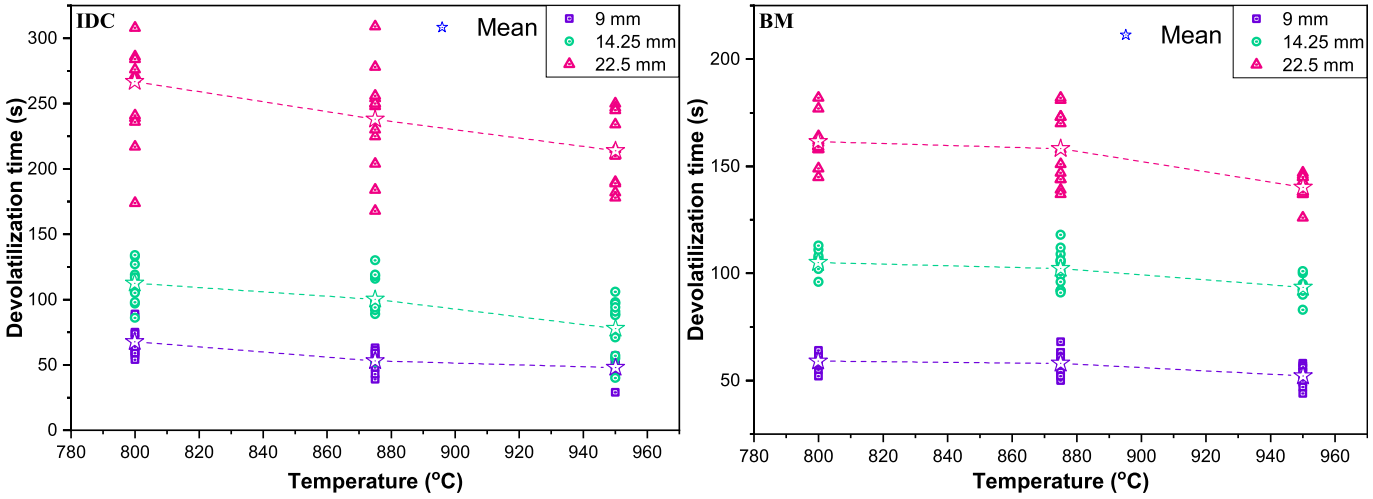

Fig. 5. Devolatilization time of IDC and BM at different bed temperatures.

volatilization reactions than the tar deposition over the sublayers of fuel particle core, at high temperatures [26,40]. Partly, crack development in the larger particles can be a cause for this reduction. Influence of bed temperature is found to be slightly more in IDC particles (reduction in the range of 15–30%) which is because of its low mineral matter.

During a fuel devolatilization, two stages are known to be present [28]. In the initial phase, low-temperature reactions occur, leading to a huge and rapid evolution of volatile matter. This phase is followed by slow reactions when the particle attains a higher temperature close to the bed, resulting in a gradual release of hydrogen [41,42]. When the particle sizes are large, these two stages overlap each other due to the temperature gradient and the devolatilization process may continue till the start of char conversion, also resulting in a longer devolatilization time. However, at higher temperatures, the rate of volatile transport out of the particle is possibly high, and thus a notable reduction in τ_d is observed in the larger sizes studied.

3.4. Effect of shape of fuel particles and fragmentation

The coal particles, when crushed before being fed to the combustors, produce particles of two groups based on shape (Fig. 6), namely (i)near-rounded and (ii)flaky. Depending upon the coal type, they produce near-rounds and flakes in various proportions viz. flakes of 26% in IC1, 34% in IC2 and 29% in IDC. Though the near-rounded ones form the larger group, it is essential to analyze the devolatilization performance of thin flakes, considering the vast quantities of coal used in thermal power stations.

The devolatilization times of the near-rounded (R)and the slender flaky (S) particles are plotted in Figs. 7–9 for IC1, IC2, and IDC, respectively. The near-rounded and slender particles produce segregated clumps of data points for all coals irrespective of particle size and bed temperature, as shown encircled in Figs. 7 and 9. For the slender fuel particles in the +20–25 mm sieve range, the mass-equivalent diameters are found in the range of 17–23 mm because of their slender forms. In the lower sieve ranges (+8–16 mm), the differences in the mass equivalent diameter of these two shape groups are relatively less.

The sphericity data of coal samples used in this study is shown in Table 5. The sphericity of near-rounded ones is in the range of 0.63–0.79, and that of thin flakes is found between 0.24 and 0.4, depending on the coal type and particle size. The τ_d of slender ones are 60% shorter (on average) than the near-rounded particles, which are 48–72% lesser in 9 mm, 52–79% in 14.25 mm, and 44–70% in 22.5 mm particles. The scatter in data points of IC2

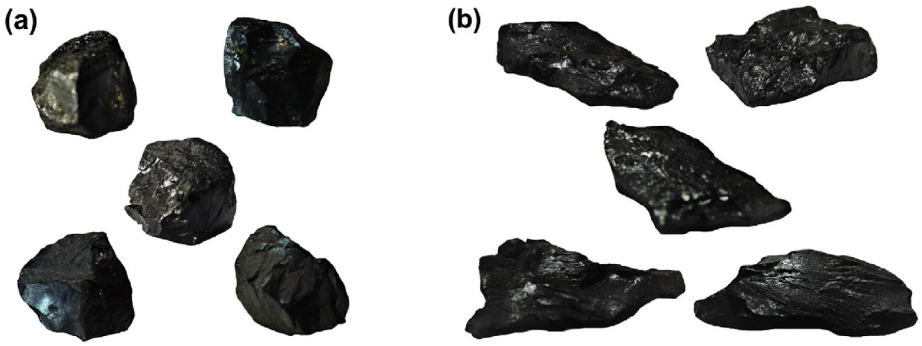

Fig. 6. IDC particles (+20–25 mm) exhibiting different shapes i.e. (a) near-rounded and (b) flaky.

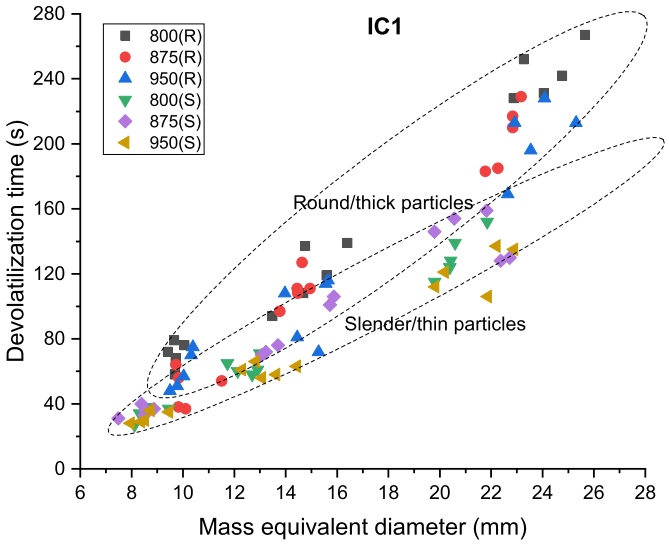

Fig. 7. Comparison of devolatilization times of near-rounded and flaky IC1 particles.

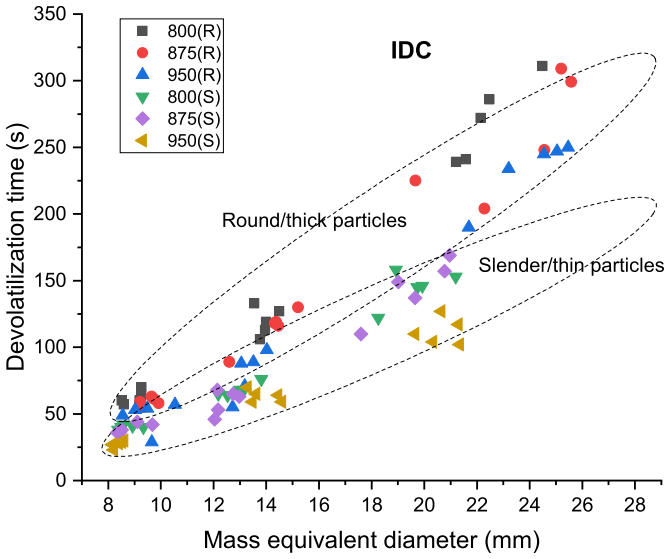

Fig. 9. Comparison of devolatilization times of near-rounded and flaky IDC particles.

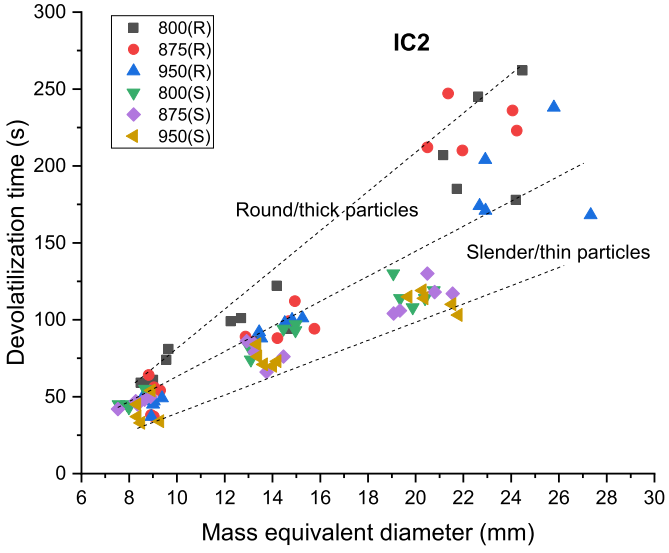

Fig. 8. Comparison of devolatilization times of near-rounded and flaky IC2 particles.

slender particles is relatively very less than in IC1 and IDC, which might be due to either very low sphericity of IC2 flakes and their relatively uniform conversion or because of low particle-comminution.

From the observations, slender flaky particles could impact the overall fuel conversion time in an industrial-scale continuous process, if their proportion in feed is significantly large. Since these particles are observed to undergo lower comminution, their particle size distributions in the later stages of conversion are less probable to change.

For understanding the effect of fragmentation on devolatilization time, the case of IC1 is considered since it is reported to fragment more compared to the other two coal types [24], resulting in widely scattered data points. Fig. 10 compares the devolatilization times obtained for fragmenting and non-fragmenting particles. The fragmented particles are found to have lesser devolatilization time than the particles that do not fragment. While the devolatilization process is in progress, the following events co-exist.

(i) Fragmentation of original fuel particle and consequent devolatilization of daughter particles at a faster rate.
(ii) Before the devolatilization is over, the daughter fragments (smaller ones) which eventually devolatilised will undergo char conversion process and may sometimes escape the reactor/basket.
(iii) The non-uniform crack formations across the particle structure, resulting in uneven conversion at different locations in the particle.

Table 5
Sphericity of coal samples tested.

Coal	+8–10 mm		+12.5–16 mm		+20–25 mm	
	Near-rounded	Slender	Near-rounded	Slender	Near-rounded	Slender
IC1	0.76	0.39	0.79	0.37	0.72	0.30
IC2	0.69	0.35	0.73	0.26	0.63	0.24
IDC	0.71	0.40	0.74	0.35	0.76	0.31

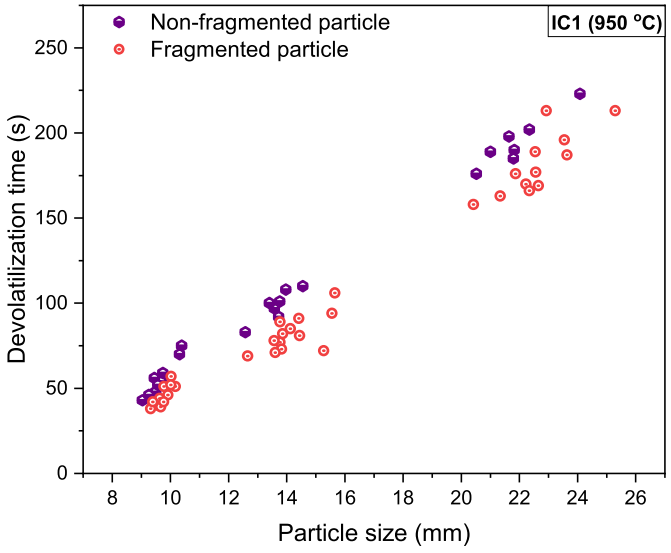

Fig. 10. Comparison of devolatilization times of fragmentating and non-fragmentating particles of IC1 at 950 °C.

All these events influence the mass loss rate, consequently bringing down the devolatilization time. Among the coals, IC2 particles which are reported to fragment lesser [24], are observed to experience further low fragmentation in their slender forms, as seen from the less dispersed data points. Fragmentation events influence the particle residence time inversely and at the same time, they enable the availability of new surfaces for the subsequent char conversion by gasification in CLC. Thus devolatilization time determination involving size changes due to fragmentation also becomes an essential measurement for CLC using large sized fuel particles.

3.5. Char yield

Char yield is defined as the percentage of the fuel mass remaining at the end of devolatilization. Char yields for the fuels studied at different operating conditions are presented in Figs. 11 and 12.

The larger particles yield more char on average than the smaller particles at the end of devolatilization, due to the carbon deposition from extensive secondary reactions occurring at high pressures [33,41,43]. So, higher char yields are possible in cases of very low volatile matter, unavailability of the porous network extending to the surface and the intraparticle secondary reactions of condensation-polymerization. The char yields of 22.5 mm particles of all fuel types are almost equal to the difference of the initial weight and the sum of proximate volatile content and moisture content. The smaller particles (+9–16 mm) show lesser char yield (below the dotted line in Figs. 11 and 12) because of one of the likely causes of particle cracking or fragmentation events and the tar cracking at high temperatures [31]. On the other hand, particles may show a high char yield than the sum of fixed carbon and ash, at lower bed temperatures.

IC2, when compared to IC1, show a comparatively lesser impact of the increase in particle size over char yield. Two probable causes for this behavior could be (i) the conversion of smaller particles of IC1 in air during the basket retrieval and quenching events (4–7s), (ii) incomplete release of volatiles from the innermost core of the larger particles. As observed from Fig. 11, IDC and BM particles do not exhibit a remarkable influence of particle size on char yield. In the course of devolatilization, IDC particles tend to expand plastically, thus aiding the volatile release without much obstruction. Similarly, biomass particles have good porosity compared to coal particles, resulting in relatively easier flow of volatiles irrespective of particle size.

With the increase in temperature, the char yield is found to decrease for all fuels, ranging from a minimum of 3% to a maximum of 48% depending on fuel type. However, this is in a bit contrary to the observation made by Borah et al. [44], where the total volatile yield is invariable at a temperature above 727 °C in conventional air environment. Also, Di Blasi and Branca [45] states that the effect of bed temperature on char yield becomes insignificant above 577 °C when devolatilised under nitrogen environment. The low char yield results in the present study can be corroborated by the char yields obtained by Xu et al. [46] in oxy-steam environment. The presence of steam atmosphere affects the char composition in terms of formation of large aromatic rings by condensation of smaller aromatic groups [46]. This process could possibly create free sites or voids in the char structure as earlier reported by Czechowski and Kidawa [47], where the formation of mesoporous structures and high surface roughness in char are noticed. This would further increase the volatile release rate at higher temperatures and as a result, shorter devolatilization times are noticed. Additionally, consumption of smaller aromatic groups is also likely, which could lead to a lower char yield. Thus, the influence of fluidizing medium on char yield is evident, and the char yield decreases with increasing bed temperatures in the iG-CLC environment. In addition, higher volatile yields and thus low char yields are favored by lesser tar deposition [26] or tar cracking in internal layers of the fuel particles at high temperatures [43]. Char yields are almost equal to their corresponding sum of fixed carbon and ash (as determined by proximate analysis) for all coals and biomass at 875 and 950 °C respectively. Char yields of BM particles are clearly well above the sum of proximate fixed carbon and ash at 800 °C, probably due to tar deposition. The yield tend to decrease with the increase in bed temperature. At 950 °C, biomass is fully devoid of carbon deposition due to the cracking of tar into lighter molecules [43].

3.6. Effect of fuel shape on char yield

Since the fuel shape influences the devolatilization time, it is more likely to affect the char yield. The char yield data points for the near-rounded (R) and slender (S) particles are populated for each coal type, and the scatter plots are shown in Fig. 13.

IC1 is the only coal type which exhibits a difference in char yield when the shape of the subjected coal particle changes (Fig. 13). The

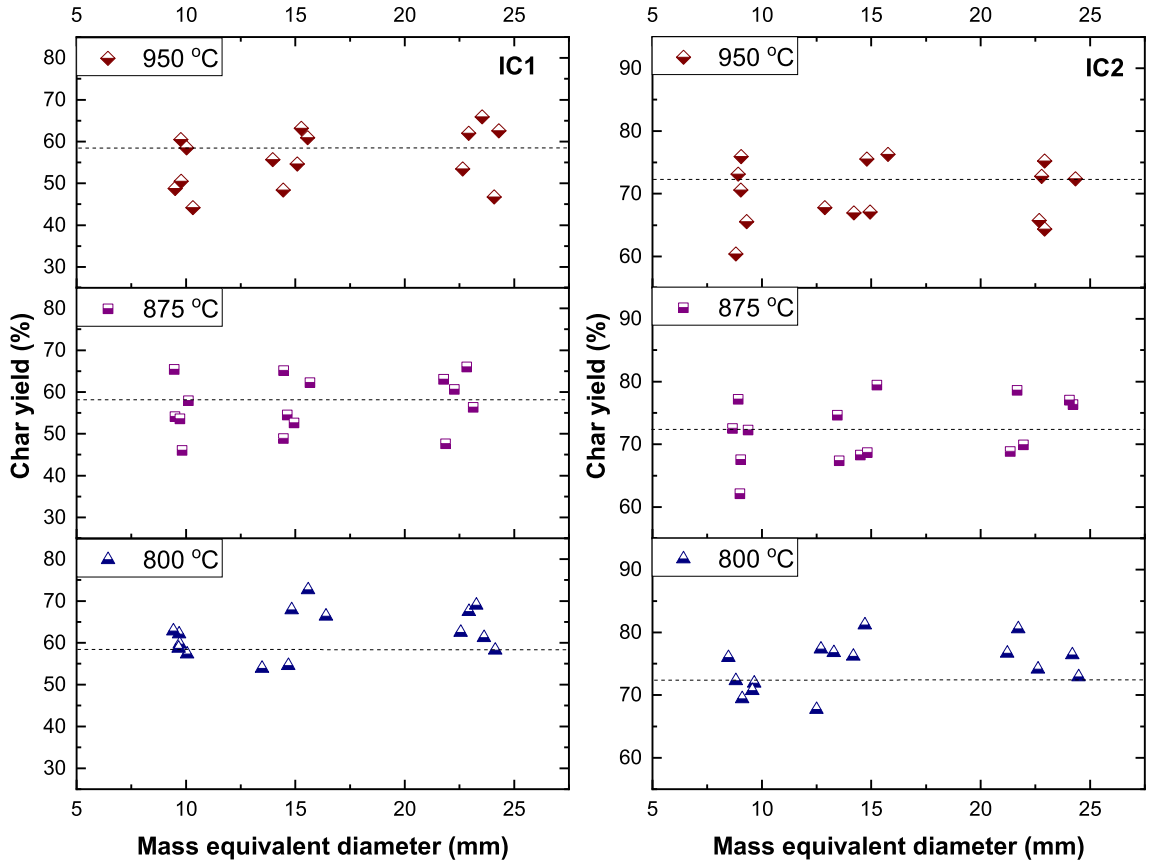

Fig. 11. Char yields of IC1 and IC2 of various particle sizes at different bed temperatures.

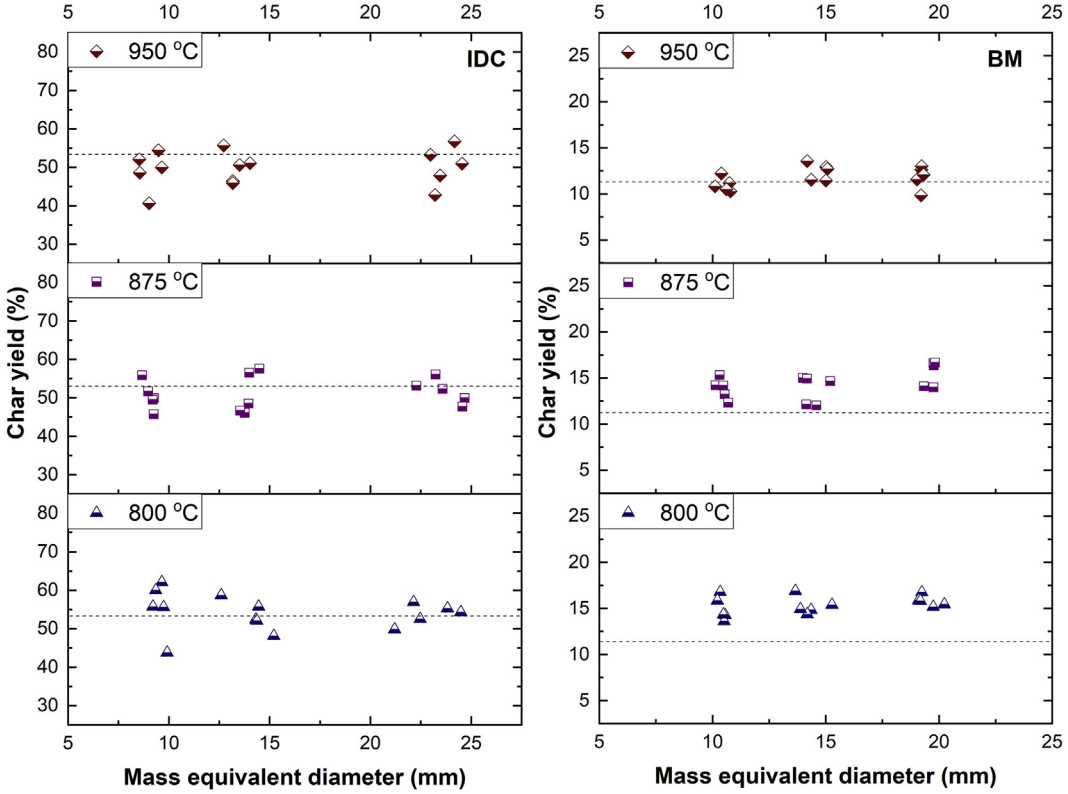

Fig. 12. Char yields of IDC and BM of various particle sizes at different bed temperatures.

primary cause could be the non-fragmenting nature of the thin flakes of IC1, unlike the near-rounded particles. The slender ones have about 15–20% higher yield of char than the near-rounded particles. In the case of IC2, this kind of observation is less probable, since the near-rounded particles themselves do not undergo extensive fragmentation [24]. Similarly, the difference in char yields between these two shapes is not noticed in IDC primarily because of the coal's plastic expansion during devolatilization regardless of the particle shape.

Influence of particle size over the char yields of Indian coal flakes is noticed, whereas, IDC shape groups are not significantly affected by size changes. As observed in near-rounded ones, the char yield of these slender species is maximum in the largest size tested. The effect of operating bed temperature is seen only in the Indonesian coal particles, i.e., char yields decrease with increase in temperature. Therefore, the shape effect on char yield depends on the fuel type studied.

3.7. Correlation of devolatilization time

For conventional combustion conditions, the correlation provided in the literature [22,48,49] represents devolatilization time as a function of only the particle size, in the form of

$$\tau_d = A.d_p^i \quad (1)$$

A new correlation embodying the effects of other parameters such as temperature and particle shape is presented in the form of

$$\tau_d = A.d_p^i.T^j.\varphi^k \quad (2)$$

where A is the proportionality constant embodying the effects of transient heat and mass transfer within the particles as well as the devolatilization kinetics [50], d_p is the particle diameter in mm, T is the operating bed temperature, and φ is the sphericity of fuel particles and i,j,k are the exponents of the respective parameters. Since cube-shaped biomass particles are only investigated in the present study, the sphericity parameter is not included during the

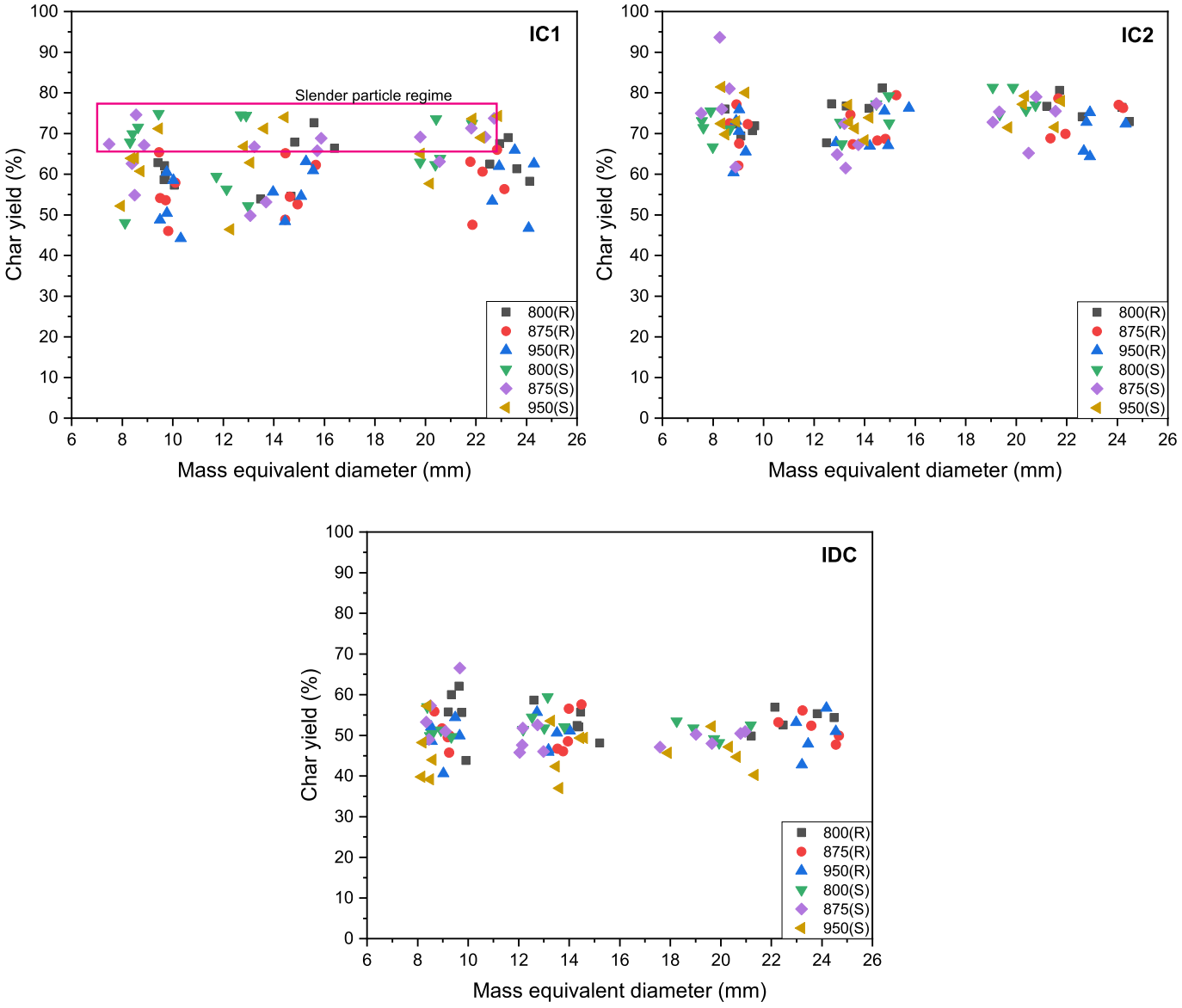

Fig. 13. Comparison of char yields of near-rounded and slender coal particles.

Table 6
Values of correlation parameters for determining devolatilization time of different fuels.

Fuels	A (Proportionality constant)	i (size factor)	j (temperature)	k (shape factor)	Coefficient of determination, R^2
IC1	2449	1.489	−1.042	0.349	0.959
IC2	19997	1.39	−1.298	0.362	0.956
IDC	9831	1.666	−1.303	0.4	0.966
BM	293	1.615	−0.799	–	0.973
All coals	10421	1.536	−1.266	0.376	0.945

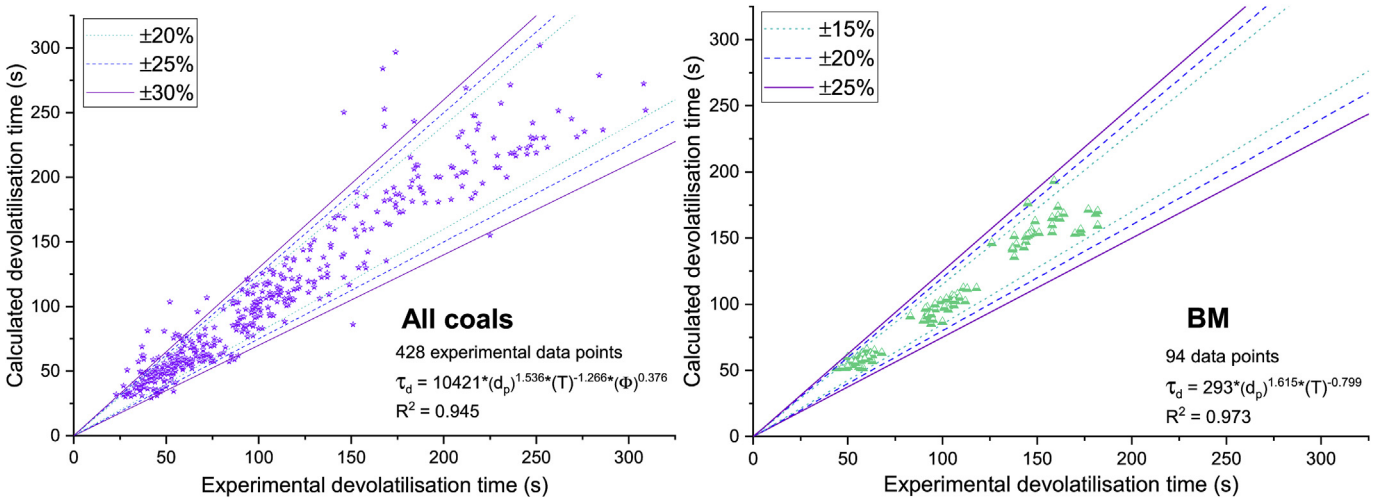

Fig. 14. Comparison of experimental and calculated values (using equation (2)) of devolatilization time of all coals and biomass.

calculation. The correlation values are given in Table 6 for all the fuels studied, which cover three particle sizes, three bed temperatures and two different particle shapes for each fuel. A generalized correlation for all the studied coal types is given as,

$$\tau_d = 10421.d_p^{1.536}.T^{-1.266}.\varphi^{0.376} \quad (3)$$

The constant A varying between 293 and 19997 seems to be an intrinsic property specific to each type of fuel and shows how strong is the intraparticular heat (and mass) transfer resistance and inversely represents the devolatilization kinetics. Indian coal IC2, which is known to have the highest density, has the highest A value and exhibits a strong negative influence of bed temperature on devolatilization time. IC1 turns out to be more reactive since its A is low amongst the coals. Biomass particles with the least A and j values have the least resistance to heat and volatile transport across the particle. Indonesian coal has the highest exponents for all the operating parameters, making it the most influenced fuel by the operating parameters. This implies that the combustion rate of IDC can be easily controlled by changing the operating conditions. The power law correlation given as equation (2) successfully fits the devolatilization times of various fuels at different operating conditions with a minimum R^2 value of 0.945. Parity plots comparing the experimental and calculated values (using equation (2)) are given as Fig. 14 for coals and biomass. About 92.5% of the calculated data points are within ±25% deviation from the experimental values. Most of the data points outside 25% deviation line are found to be overestimated values by the correlation, particularly for the +8−10 mm size range. Calculated values for larger particles are found to match well with the experimental data points.

For devolatilization conditions in air, Prins et al. [51] states that earlier researchers defined 'i' values varying from 0.3 to 1.8, whereas Agarwal et al. [52] defines i = 2 (i.e. d_p^2) for coal particles larger than 1 mm and later they recognized that d_p^2 relation can be applied only for the case of external heat transfer controlled devolatilization. As commonly reported, the exponents of particle size ('i') in CLC conditions are found in the range of 1.39−1.66. The values of intrinsic constant 'A' for conventional air combustion studies range between 1 and 6 [20,50]. Since other influencing parameters such as temperature and sphericity are incorporated in the present correlation and the tested environment is CLC, 'A' becomes a very sensitive and large value (specific to fuel type) among other correlation parameters. Calculated devolatilization times of biomass particles match very closely with measured values, i.e., more than 95% of the values lie within ±15% deviation zone. Thus, particle size is the most influencing parameter followed by operating bed temperature and sphericity, in order.

4. Conclusions

With the use of large fuel particles (mm-sized) in CLC, the particle residence times are improved thereby reducing the carryover of unconverted char into the air reactor. Devolatilization time or the rate of devolatilization determines the oxygen carrier demand in fuel reactor, as the release of combustible volatiles is the fastest step in the solid fuel conversion. With the additional aid of fragmentation data and the char conversion times, the largest size of a particular fuel for its application in continuous CLC process can be established.

The results of the present study show that the devolatilization time is found to increase with the increase in particle size and decrease with increase in operating bed temperature, analogous to the behavior observed in the conventional fluidized bed combustion. The devolatilization times of Indonesian coal are the highest among the coals studied, with biomass particles having the least devolatilization times. It is the most influenced fuel type, by the changes in operating parameters because of its highest combustible

matter composition. Coal flakes are found to have 60% lesser devolatilization time than the near-rounded particles, indicating the importance of the shape effect to be considered in modeling of devolatilization and design of FB-CLC system. Char yield is lowest at 950 °C irrespective of the particle size and sphericity. Larger coal particles always have higher char yields than the smaller particles, whereas char yields of biomass particles do not show significant changes. Correlations for devolatilization time of coals and biomass particles in CLC conditions are arrived, with a satisfactory value of the coefficient of determination of around 0.95. Particle size is the most influencing parameter of devolatilization and sphericity being the least. Based on the fuel nature and primary fragmentation behavior, the more reactive fuels (i.e. with high volatile matter and low ash) like biomass, Indonesian coal and IC1(to a certain extent) can be comfortably used in larger sizes, whereas IC2 (high ash nature) has to be considered for usage in their lower and mid-range sizes used in this study.

Acknowledgments

We wish to thank Prof. G. Srinikethan, Department of Chemical Engineering, NITK Surathkal for his support in sourcing iron ore from M/s SLR Metaliks Ltd., Bellary, Karnataka. Thanks to M/s Udupi Power Corporation Limited for helping us with Indonesian coal for our work and SAIF, IIT Bombay for carrying out the ultimate analyses for the fuels used in this study.

References

[1] J. Gibbins, H. Chalmers, Carbon capture and storage, Energy Policy 36 (2008) 4317–4322, https://doi.org/10.1016/j.enpol.2008.09.058.
[2] B.P. Spigarelli, S.K. Kawatra, Opportunities and challenges in carbon dioxide capture, J. CO2 Util. 1 (2013) 69–87, https://doi.org/10.1016/j.jcou.2013.03.002.
[3] B. Sreenivasulu, D.V. Gayatri, I. Sreedhar, K.V. Raghavan, A journey into the process and engineering aspects of carbon capture technologies, Renew. Sustain. Energy Rev. 41 (2015) 1324–1350, https://doi.org/10.1016/j.rser.2014.09.029.
[4] J. Adánez, A. Abad, T. Mendiara, P. Gayán, L.F. de Diego, F. García-Labiano, Chemical looping combustion of solid fuels, Prog. Energy Combust. Sci. 65 (2018) 6–66, https://doi.org/10.1016/j.pecs.2017.07.005.
[5] T. Mattisson, M. Keller, C. Linderholm, P. Moldenhauer, M. Rydén, H. Leion, A. Lyngfelt, Chemical-looping technologies using circulating fluidized bed systems: status of development, Fuel Process. Technol. 172 (2018) 1–12, https://doi.org/10.1016/j.fuproc.2017.11.016.
[6] A. Nandy, C. Loha, S. Gu, P. Sarkar, M.K. Karmakar, P.K. Chatterjee, Present status and overview of chemical looping combustion technology, Renew. Sustain. Energy Rev. 59 (2016) 597–619, https://doi.org/10.1016/j.rser.2016.01.003.
[7] J. Ströhle, M. Orth, B. Epple, J. Stroehle, M. Orth, B. Epple, J. Strï¿½hle, M. Orth, B. Epple, Chemical looping combustion of hard coal in a 1 MW_{th} pilot plant using ilmenite as oxygen carrier, Appl. Energy 157 (2015) 288–294, https://doi.org/10.1016/j.apenergy.2015.06.035.
[8] A. Lyngfelt, Chemical-looping combustion of solid fuels - status of development, Appl. Energy 113 (2014) 1869–1873, https://doi.org/10.1016/j.apenergy.2013.05.043.
[9] P. Basu, Combustion and Gasification in Fluidized Beds, CRC Press, 2006, https://doi.org/10.1017/CBO9781107415324.004.
[10] L.-S. Fan, L. Zeng, W. Wang, S. Luo, Chemical looping processes for CO2 capture and carbonaceous fuel conversion – prospect and opportunity, Energy Environ. Sci. 5 (2012) 7254, https://doi.org/10.1039/c2ee03198a.
[11] N. Berguerand, A. Lyngfelt, Chemical-looping combustion of petroleum coke using ilmenite in a 10 kwth unit-high-temperature operation, Energy Fuels 23 (2009) 5257–5268, https://doi.org/10.1021/ef900464j.
[12] G. Huijun, S. Laihong, F. Fei, J. Shouxi, Experiments on biomass gasification using chemical looping with nickel-based oxygen carrier in a 25 kWth reactor, Appl. Therm. Eng. 85 (2015) 52–60, https://doi.org/10.1016/j.applthermaleng.2015.03.082.
[13] J. Adanez, A. Abad, F. Garcia-Labiano, P. Gayan, L.F. de Diego, Progress in chemical-looping combustion and reforming technologies, Prog. Energy Combust. Sci. 38 (2012) 215–282, https://doi.org/10.1016/j.pecs.2011.09.001.
[14] H. Leion, T. Mattisson, A. Lyngfelt, Using chemical-looping with oxygen uncoupling (CLOU) for combustion of six different solid fuels, Energy Procedia 1 (2009) 447–453, https://doi.org/10.1016/j.egypro.2009.01.060.
[15] N. Berguerand, A. Lyngfelt, Design and operation of a 10kWth chemical-looping combustor for solid fuels – testing with South African coal, Fuel 87 (2008) 2713–2726, https://doi.org/10.1016/j.fuel.2008.03.008.
[16] P. Ohlemüller, J.-P. Busch, M. Reitz, J. Ströhle, B. Epple, Chemical-looping combustion of hard coal: autothermal operation of a 1 MW th pilot plant, J. Energy Resour. Technol. 138 (2016), 042203, https://doi.org/10.1115/1.4032357.
[17] L. Jia, H.A. Becker, R.K. Code, Devolatilization and char burning of coal particles in a fluidized bed combustor, Can. J. Chem. Eng. 71 (1993) 10–19, https://doi.org/10.1002/cjce.5450710103.
[18] N. Berguerand, A. Lyngfelt, T. Mattisson, P. Markström, Chemical looping combustion of solid fuels in a 10 kW th unit, Oil Gas Sci. Technol. – Rev. d'IFP Energies Nouv. 66 (2011) 181–191, https://doi.org/10.2516/ogst/2010023.
[19] P.K. Agarwal, W.E. Genetti, Y.Y. Lee, Pradeep K. Agarwal, W.E. Genetti, Y.Y. Lee, Model for devolatilizaion of coal particles in fluidized beds, Fuel 63 (1984) 1157–1165, https://doi.org/10.1016/0016-2361(84)90205-9.
[20] J.F.F. Stubington, T.Y.S.Y.S. Chui, S. Saisithidej, Experimental factors affecting coal devolatilization time in fluidized bed combustion, Fuel Sci. Technol. Int. 10 (1992) 397–419, https://doi.org/10.1080/08843759208915997.
[21] D. Sasongko, J.F. Stubington, Significant factors affecting devolatilization of fragmenting, non-swelling coals in fluidized bed combustion, Chem. Eng. Sci. 51 (1996) 3909–3918, https://doi.org/10.1016/0009-2509(96)00242-4.
[22] D.P.P. Ross, C.A. Heidenreich, D.K. Zhang, Devolatilisation times of coal particles in a fluidised-bed, Fuel 79 (2000) 873–883, https://doi.org/10.1016/S0016-2361(99)00227-6.
[23] H. Jüntgen, K.H. Van Heek, An update of German non-isothermal coal pyrolysis work, Fuel Process. Technol. 2 (1979) 261–293, https://doi.org/10.1016/0378-3820(79)90018-3.
[24] K.S. Pragadeesh, D.R. Sudhakar, Primary fragmentation behavior of Indian coals and biomass during chemical looping combustion, Energy Fuels 32 (2018) 6330–6346, https://doi.org/10.1021/acs.energyfuels.8b00640.
[25] K.S. Pragadeesh, D.R. Sudhakar, Color indistinction method for the determination of devolatilization time of large fuel particles in chemical looping combustion, Energy Fuels 33 (2019) 4542–4551, https://doi.org/10.1021/acs.energyfuels.8b04310.
[26] A. Bliek, W.M. Van Poelje, W.P.M. Van Swaaij, F.P.H. Van Beckum, Effects of intraparticle heat and mass transfer during devolatilization of a single coal particle, AIChE J. 31 (1985) 1666–1681, https://doi.org/10.1002/aic.690311010.
[27] M.K. Urkan, M. Arikol, Burning times of volatiles from Turkish coals during fluidized bed combustion, Fuel 73 (1994) 768–772, https://doi.org/10.1016/0016-2361(94)90022-1.
[28] S. Oka, Fluidized Bed Combustion, CRC press, 2003.
[29] J. Tomeczek, H. Palugniok, Specific heat capacity and enthalpy of coal pyrolysis at elevated temperatures, Fuel 75 (1996) 1089–1093, https://doi.org/10.1016/0016-2361(96)00067-1.
[30] K. Jayaraman, I. Gokalp, Thermogravimetric and evolved gas analyses of high ash Indian and Turkish coal pyrolysis and gasification, J. Therm. Anal. Calorim. 121 (2015) 919–927, https://doi.org/10.1007/s10973-015-4500-9.
[31] J.F. Stubington, Sumaryono, Release of volatiles from large coal particles in a hot fluidized bed, Fuel 63 (1984) 1013–1019, https://doi.org/10.1016/0016-2361(84)90327-2.
[32] D.B. Anthony, J.B. Howard, Coal devolatilization and hydrogastification, AIChE J. 22 (1976) 625–656, https://doi.org/10.1002/aic.690220403.
[33] J. Khan, T. Wang, Implementation of a demoisturization and devolatilization model in multi-phase simulation of a hybrid entrained-flow and fluidized bed mild gasifier, Int. J. Clean Coal Energy (2013) 35–53, https://doi.org/10.4236/ijcce.2013.23005, 02.
[34] R.C. Borah, P.G. Rao, P. Ghosh, Devolatilization of coals of northeastern India in inert atmosphere and in air under fluidized bed conditions, Fuel Process. Technol. 91 (2010) 9–16, https://doi.org/10.1016/j.fuproc.2009.08.014.
[35] H. Ge, L. Shen, H. Gu, T. Song, S. Jiang, Combustion performance and sodium transformation of high-sodium ZhunDong coal during chemical looping combustion with hematite as oxygen carrier, Fuel 159 (2015) 107–117, https://doi.org/10.1016/j.fuel.2015.06.073.
[36] H. Stainton, A. Ginet, K. Surla, A. Hoteit, Experimental investigation of CLC coal combustion with nickel based particles in a fluidized bed, Fuel 101 (2012) 205–214, https://doi.org/10.1016/j.fuel.2011.08.025.
[37] T. Mattisson, D. Jing, A. Lyngfelt, M. Rydén, Experimental investigation of binary and ternary combined manganese oxides for chemical-looping with oxygen uncoupling (CLOU), Fuel 164 (2016) 228–236, https://doi.org/10.1016/j.fuel.2015.09.053.
[38] S. Niksa, L.E. Heyd, W.B. Russel, D.A. Saville, On the role of heating rate in rapid coal devolatilization, Symp. Combust. 20 (1985) 1445–1453, https://doi.org/10.1016/S0082-0784(85)80637-8.
[39] R.M. Morris, Effect of particle size and temperature on evolution rate of volatiles from coal, J. Anal. Appl. Pyrolysis 27 (1993) 97–107, https://doi.org/10.1016/0165-2370(93)80001-G.
[40] H. Kobayashi, J.B. Howard, A.F. Sarofim, Coal devolatilization at high temperatures, Symp. Combust. 16 (1977) 411–425, https://doi.org/10.1016/S0082-0784(77)80341-X.
[41] S.C. Saxena, Devolatilization and combustion characteristics of coal particles, Prog. Energy Combust. Sci. 16 (1990) 55–94, https://doi.org/10.1016/0360-1285(90)90025-X.
[42] J.P. Morris, D.L. Keairns, Coal devolatilization studies in support of the Westinghouse fluidized-bed coal gasification process, Fuel 58 (1979) 465–471, https://doi.org/10.1016/0016-2361(79)90089-9.

[43] Y.B. Yang, V.N. Sharifi, J. Swithenbank, L. Ma, L.I. Darvell, J.M. Jones, M. Pourkashanian, A. Williams, Combustion of a single particle of biomass, Energy Fuels 22 (2008) 306–316, https://doi.org/10.1021/ef700305r.
[44] R.C. Borah, P. Ghosh, P.G. Rao, A review on devolatilization of coal in fluidized bed, Int. J. Energy Res. 35 (2011) 929–963, https://doi.org/10.1002/er.1833.
[45] C. Di Blasi, C. Branca, Temperatures of wood particles in a hot sand bed fluidized by nitrogen, Energy Fuels 17 (2003) 247–254, https://doi.org/10.1021/ef020146e.
[46] J. Xu, S. Su, Z. Sun, M. Qing, Z. Xiong, Y. Wang, L. Jiang, S. Hu, J. Xiang, Effects of steam and CO2 on the characteristics of chars during devolatilization in oxy-steam combustion process, Appl. Energy 182 (2016) 20–28, https://doi.org/10.1016/j.apenergy.2016.08.121.
[47] F. Czechowski, H. Kidawa, Reactivity and susceptibility to porosity development of coal maceral chars on steam and carbon dioxide gasification, Fuel Process. Technol. 29 (1991) 57–73, https://doi.org/10.1016/0378-3820(91)90017-7.
[48] J.F. Stubington, T.M. Linjewile, The effects of fragmentation on devolatilization of large coal particles, Fuel 68 (1989) 155–160, https://doi.org/10.1016/0016-2361(89)90316-5.
[49] J.Q. Zhang, H.A. Becker, R.K. Code, Devolatilization and combustion of large coal particles in a fluidized bed, Can. J. Chem. Eng. 68 (1990) 1010–1017, https://doi.org/10.1002/cjce.5450680617.
[50] R. Solimene, R. Chirone, P. Salatino, Characterization of the devolatilization rate of solid fuels in fluidized beds by time-resolved pressure measurements, AIChE J. 58 (2012) 632–645, https://doi.org/10.1002/aic.12607.
[51] W. Prins, R. Siemons, W.P.M.M. Van Swaaij, M. Radovanovic, Devolatilization and ignition of coal particles in a two-dimensional fluidized bed, Combust. Flame 75 (1989) 57–79, https://doi.org/10.1016/0010-2180(89)90087-4.
[52] P.K. Agarwal, W.E. Genetti, Y.Y. Lee, Model for devolatilization of coal particles in fluidized beds, Fuel 63 (1984) 1157–1165, https://doi.org/10.1016/0016-2361(84)90205-9.